T2R2 東京科学大学 リサーチリポジトリ
Science Tokyo Research Repository

論文 / 著書情報
Article / Book Information

Title	Bundled Wire Drive: Proposal and Feasibility Study of a Novel Tendon-Driven Mechanism Using Synthetic Fiber Ropes
Authors	Gen Endo, Youki Wakabayashi, Hiroyuki Nabae, Koichi Suzumori
Citation	IEEE Robotics and Automation Letters (RAL), Vol. 4, Issue 2, pp. 966-972
Pub. date	2019, 1
Copyright	(c) 2019 IEEE. Personal use of this material is permitted. Permission from IEEE must be obtained for all other uses, in any current or future media, including reprinting/republishing this material for advertising or promotional purposes, creating new collective works, for resale or redistribution to servers or lists, or reuse of any copyrighted component of this work in other works.
DOI	https://dx.doi.org/10.1109/LRA.2019.2893429
Note	This file is author (final) version.

Powered by T2R2 (Science Tokyo Research Repository)

Bundled Wire Drive: Proposal and Feasibility Study of a Novel Tendon-Driven Mechanism Using Synthetic Fiber Ropes

Gen Endo[1], Youki Wakabayashi[1], Hiroyuki Nabae[1] and Koichi Suzumori[1]

***Abstract*—This paper proposes a new wire-driven mechanism in order to relay many ropes very simply and compactly. Ropes pass through in a joint while bundled. Synthetic fiber rope can slide and twist, exploiting its low friction coefficient. In order to use this mechanism, it is necessary to investigate the influence of sliding on tension transmission efficiency and rope strength. The results of this study reveal that it is feasible for a robot arm using this mechanism to have more than 15 joints. Sliding has little influence on rope strength. The feasibility of this system was studied through hardware experiments and its mechanical performance was evaluated by constructing a horizontally extendable manipulator with three degrees of freedom.**

***Index Terms*—Tendon/Wire Mechanism, Mechanism Design, Redundant Robots, Synthetic Fiber Rope**

I. INTRODUCTION

WIRE-DRIVEN mechanisms have many advantages including 1) light weight, 2) low cost, and 3) high flexibility in mechanical design. In regard to mechanical design, wire-driven mechanisms can transmit actuation power from an actuator to a driven joint located at a long distance from the actuator. In reality, the human body has been intensively exploiting wire- (tendon-) driven mechanisms for efficient joint actuations and optimal muscle location throughout the evolution process. Given the design flexibility of the actuator's location, this characteristic allows robot designers to design compact and efficient mechanisms such as dexterous robotic hands (Fig. 1(a)) [1] and laparoscopic surgical systems [2]. Moreover, wire-driven mechanisms can achieve an extremely large motion range by winding up the wire such as in the case of a crane and an elevator.

In regard to the material of the wire, synthetic fiber ropes have been the focus of many studies because of their high tensile strength, high flexibility, low weight, and low friction. The maximum tensile strength of a synthetic fiber rope is about 2.3 times higher than that of a conventional stainless steel wire rope, whereas its weight and friction coefficient are 1/8th and 1/5th of its conventional counterpart, respectively. Thus, if we were to fully exploit these advantages of synthetic fiber ropes, it may be possible to develop a high performance robot, which is not feasible with conventional mechanisms. In our previous works, we investigated modeling of synthetic fiber ropes [3], tensile strength degradation by bending [4], repetitive bending durability [5], and the terminal fixation method [6].

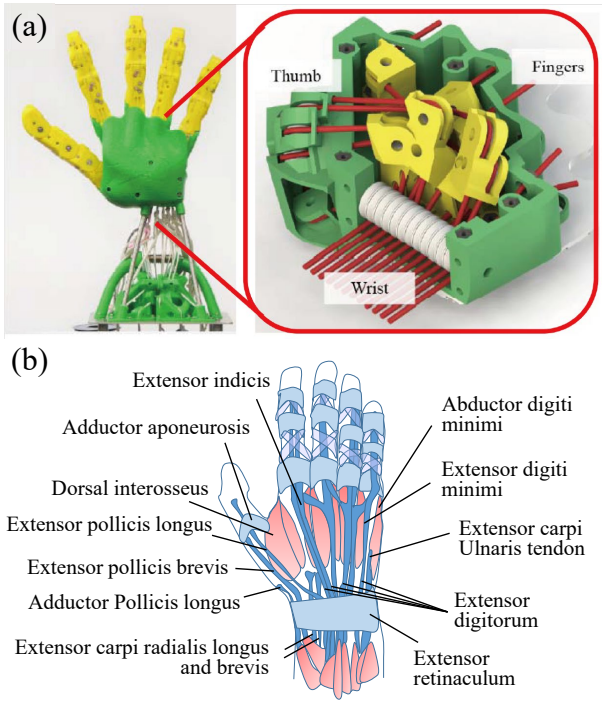

Fig. 1. Robotic hand in [1] and human hand

In this paper, we focus on the small friction coefficient of the synthetic fiber rope. We propose a novel wire-driven mechanism using synthetic fiber ropes inspired by a human hand (Fig. 1(b)). The proposed mechanism utilizes multiple synthetic fiber ropes to drive multiple degrees of freedom. The ropes are bundled and share the same transmitting pathway to achieve a simple and compact mechanism. The schematics of this concept are shown in Fig. 2. If we use conventional metal wires, the proposed mechanism may not work due to

Manuscript received: September, 10, 2018; Revised November, 6, 2018; Accepted December, 29, 2018.

This paper was recommended for publication by Editor Paolo Rocco upon evaluation of the Associate Editor and Reviewers' comments.

*This work was supported by the New Energy and Industrial Technology Development Organization (NEDO).

[1]All authors are with the Department of Mechanical Engineering, Tokyo Institute of Technology, 2-12-1 Ookayama, Meguro-ku, Tokyo 152-8550, Japan endo.g.aa at m.titech.ac.jp

Digital Object Identifier (DOI) : see top of this page.

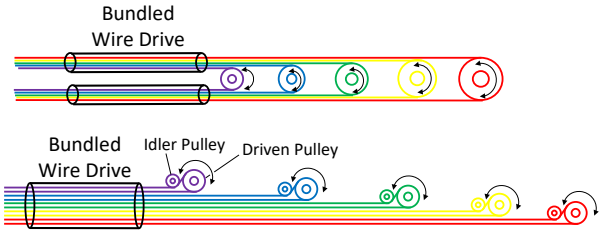

Fig. 2. Basic concept of bundled wire drive

high friction coefficient of the metal wires. In contrast, with synthetic fiber rope, we can allow multiple ropes to collide and slide with/along each other, exploiting their low frictional coefficients.

Our goals in this paper are to propose a new wire-driven mechanism named "Bundled Wire Drive," study its feasibility through hardware experiments, and evaluate its mechanical performance by constructing a horizontally extendable three-degree-of-freedom (DoF) manipulator.

The rest of this paper is organized as follows. Section II presents the bundled wire drive design, and Section III investigates its tension transmission efficiency using a DoF experimental apparatus. Section IV discusses the durability of the synthetic fiber rope, and Section V evaluates the effectiveness of the proposed mechanism by developing a three-DoF manipulator. Section VI concludes this paper and discusses future work.

II. PROPOSAL OF BUNDLED WIRE DRIVE

It is recognized that the friction coefficient of a steel wire rope on a steel pulley is approximately 0.3, which is relatively high. A large friction force is exerted when multiple wires are in sliding contact because the surface of the wire rope is uneven due to the combined and twisted strands. Therefore, conventional wire-driven mechanisms using metal wire ropes usually avoid sliding contact and collision of wires as much as possible by introducing multiple passive pulleys to ensure clear wire routes. Although tension transmission efficiency can be maximized by using freely rotating multiple passive pulleys, the wire-driving mechanism tends to be bulky and very complicated. Treratanakulwong et al. [1] (see Fig. 1(a)) tried to ensure no contact between wires, and optimized the locations of the pulleys, which resulted in a complicated structure and an increase in the number of parts.

In contrast, the human hand shown in Fig. 1(b) has multiple tendons to drive the fingers, and the tendons are bundled by carpal ligaments and connected to the muscles located in the forearm. Hence, this anatomical structure allows the bundling of tendons and their sliding against each other, which consequently achieves a very compact and simple mechanism.

Inspired by this structure, we propose a novel wire-driven mechanism called "Bundled Wire Drive (BWD)." We utilize multiple synthetic fiber ropes with low friction coefficients to drive multiple DoF, and bundle them together, allowing sliding against each other. The BWD can be a compact and simple structure with a reduced parts count because multiple ropes can share the same wire route. The conceptual schematic

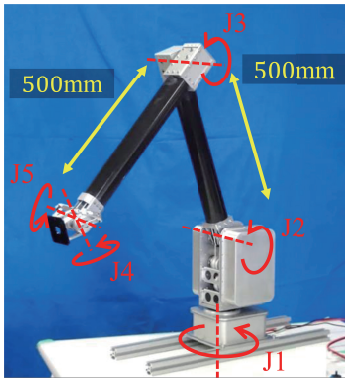

Fig. 3. 5-DoF light duty arm [11]: the three distal joints (J3, J4, and J5) are driven by wires, and their actuators are installed in the square-shaped boxes.

figures are shown in Fig. 2. The ropes colored by each DoF are bundled and slide through the black cylinders. A conduit cable can serve the purpose of the black cylinders. If we install idler pulleys close to the output pulleys, we can save more space by bundling all the ropes. Thus, the BWD is a very simple and compact wire-driving mechanism.

The literature survey indicates some similar approaches that allow wires to contact and/or slide against one another. For instance the Twisted String Actuator generates a compression force by twisting two or more synthetic fiber strings [7][8]. Nakamoto et al. designed a 7-DoF wire-driven humanoid arm, and the wires for distal joints were squeezed at a proximal link in order to locate them close to the endorotation axis in the arm [9]. OC robotics developed wire-driven snake-like manipulators, where the driving wires slid through segmented structural parts [10]. However, to the best of our knowledge, none of these studies have explored multiple driving wires that explicitly share the same wire routing.

Despite its mechanical design advantages, however, there are some concerns about the feasibility and effectiveness of this mechanism, such as transmission efficiency, durability against repetitive sliding, and interference between each DoF. In order to discuss the feasibility of the BWD, we investigate a wire-driven rotating joint with an offset in the axial direction, as shown in Fig. 3 in this paper. Joint 3, 4, and 5 are driven by wires, and their actuators are mounted on the base structure. Due to an offset, J3 has a large range of motion, namely, ± 170 deg. The wires for J4 and J5 must go through J3.

Figure 4 shows design candidates for J3, where the driving wires for J3 are sky blue, and the relayed wires for J4 and J5 are red and orange, respectively. Figure 4(a) shows a conventional design for J3 using torque tubes (bearing supported coaxial pipes). This mechanism can efficiently transmit actuator power because of rotational bearing. However, additional wire tensioners are required for J4 and J5, increasing the mechanism's complexity. Figure 4(b) utilizes relay pulleys to locate relayed wires close to the axis of J3, similar to [9]. This design can also achieve high transmission efficiency, but an additional eight pulleys are required. Moreover, it is difficult to increase the number of relayed wires in this solution, because

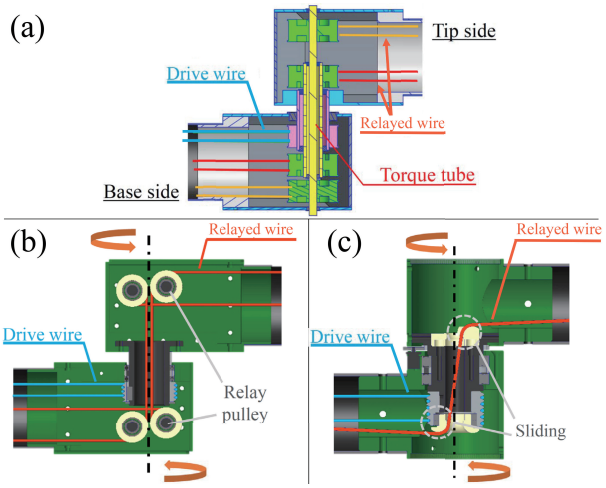

Fig. 4. Wire-driven rotational joint with an offset in the axial direction (J3): (a) conventional mechanism using torque tubes, (b) twisting relay, and (c) bundled wire drive

it is difficult to install many relay pulleys in the limited space in J3. Therefore, if the relayed wires can share the same pathways, as is the case in the BWD, the joint mechanism can be much simpler, as shown in Fig. 4(c). This mechanism also has scalability in terms of the number of distal joints.

In the following sections, we investigate the feasibility and effectiveness of the BWD mechanism shown in Fig. 4(c).

III. TENSION TRANSMISSION EFFICIENCY

In this section, we discuss reduction in the tension transmission efficiency due to friction that occurs when the rope slides against the surface. It is possible to estimate the feasible number of joints in the long-reach arms by measuring the decrease in the tension transmission efficiency.

A. Experimental Setup

Figure 5 shows the sectional and top views of the experimental device. As seen in Fig. 5a, the device consists of three parts: base (black), upper arm (blue), and lower arm (red). Since these are assembled using bearings, each of them can rotate freely. Therefore, the ropes are twisted in the middle when the joint rotates, but radial sliding does not occur because the relative positions of the ropes and the sliding surfaces in both the upper and lower sections remain unchanged. The axial sliding of the rope relayed to pass from the lower to the upper part of the joint occurs, as denoted by the dotted red circles shown in Fig. 5a. The upper arm is rotationally driven around the vertical axis by a timing belt. The curvature of the joint sliding surface is set to R = 20 mm so as not to cause strength reductions in the ropes by bending [4]. The material of the sliding surfaces in contact with the rope is made of POM, and UHMWPE fiber rope (Hayami Industry Co., DB-96HSL, diameter 2 mm) was used. This experiment uses a one-joint model mechanism, as shown in Fig. 6. Tension T1 and T2, before and after passing through the joint, respectively, is measured by the load cell (LUR-A-SA1, KYOWA) when stretching the ropes using tensioners.

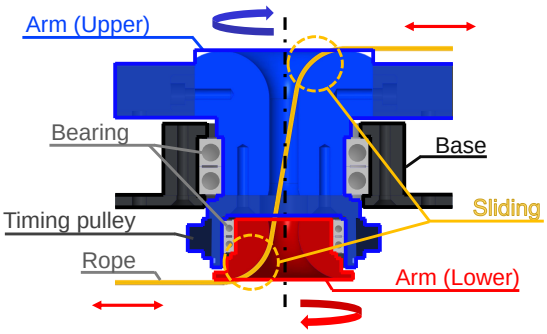

(a) Sectional view.

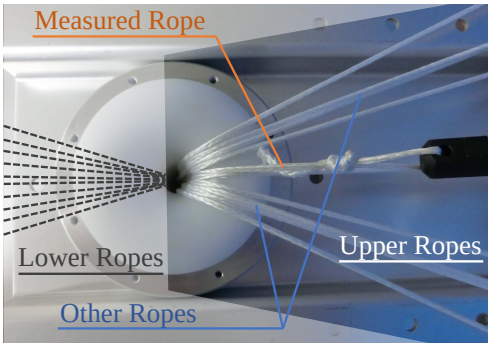

(b) Top view.

Fig. 5. Experimental device to measure the influence of allowing axial sliding of ropes on tension.

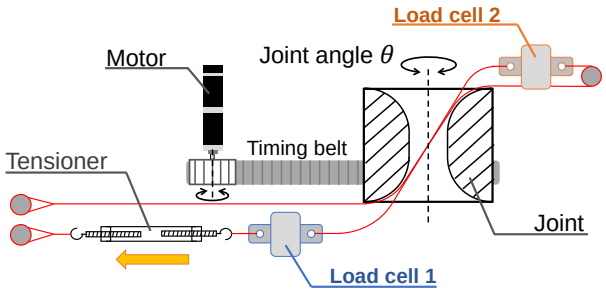

Fig. 6. System of experiment to investigate influence of allowing axial sliding of ropes on tension.

B. Experiment Results

The tension transmission efficiency was measured when the joint angle and number of ropes passing through the joint were varied. Tension transmission efficiency η_T is defined by the following equation.

$$\eta_T(\theta, n) = \frac{T_2}{T_1}. \tag{1}$$

θ is the angle of the joint and n is the number of ropes passing through the joint. Fig. 7 shows the obtained results. The tension transmission efficiency decreases as the joint angle and number of ropes passing through the joint increase. This is considered to be caused by interference between the ropes due to their twisting. We only discuss the case in which the joint angle is π because tension transmission efficiency is the lowest in this case. The relationship between the number of

ropes and tension transmission efficiency η_T for the chosen joint angle is approximated by the following equation.

$$\eta_T(\pi, n) = -0.0120n + 0.901. \tag{2}$$

Let us think about a serially connected long-reach manipulator using the proposed joints. When considering robot arms having k joints, as shown in Fig. 8, the tension transmission efficiency becomes $\eta_T(\pi, 2k-2i-2)$ because $2k-2i-2$ ropes are passed through the i-th joint counted from the base. Since the tension transmission efficiency of the rope that drives the tip joint $\eta_{\mathrm{Tip}}(k)$ can be expressed by the product of the tension transmission efficiency of the joint through, it can be obtained from the following expression.

$$\eta_{\mathrm{Tip}}(k) = \prod_{i=0}^{k-1} \eta_T(\pi, 2k-2i-2) \tag{3}$$

$$= \prod_{i=0}^{k-1} \{-0.0240(k-i-1) + 0.901\}. \tag{4}$$

Fig. 9 shows the relationship between the number of joints k and the tension transmission rate at the tip $\eta_{\mathrm{Tip}}(k)$. Assuming that the tension of the rope required at the tip is 40 N, and the strength of the used ropes is 4.3 kN, the necessary tension transmission efficiency is approximately 1.0%. Therefore, the feasible number of joints in the robot arm using the proposed mechanism is estimated as 15.

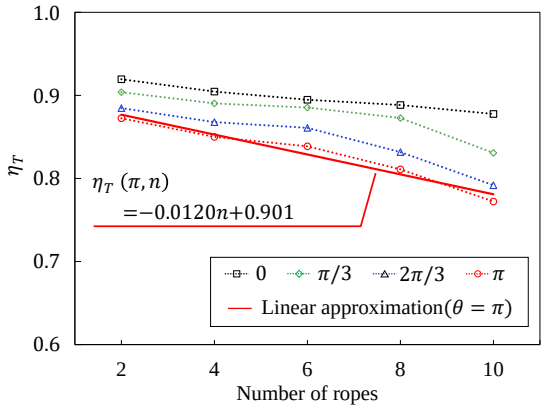

Fig. 7. Relationship between number of ropes and tension transmission rate.

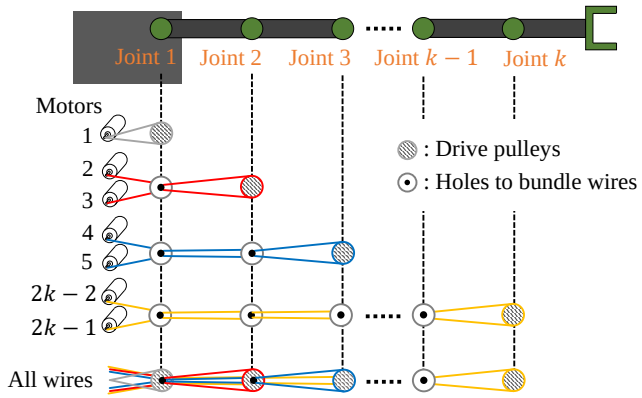

Fig. 8. Arrangement of tendons, holes, and pulleys of the arm.

IV. TENDON DURABILITY

In this section, we discuss the durability against the sliding of the rope. By investigating this aspect, we show that the hardware using the proposed mechanism can endure operation for a long time.

A. Experimental Setup

To investigate the decrease in the strength of the rope due to sliding, we slide the rope through the fixed pulley and it undergoes repeated bending, as shown in Fig. 10. The test pulleys are made of POM and are fixed to avoid rotation. The rope is repeatedly slid and bent, with constant tension being generated by the weight. The detailed experimental conditions are described in ISO 2020:1997 (note that the test pulley is free to rotate in this case). However, the repeat speed of the experiment is set to 25% of the standard. The strength of the rope after repeated sliding is measured by tensile tests. By comparing the strength after repetitive sliding against the tensile strength of the virgin rope, the reduction in rope strength due to sliding is evaluated.

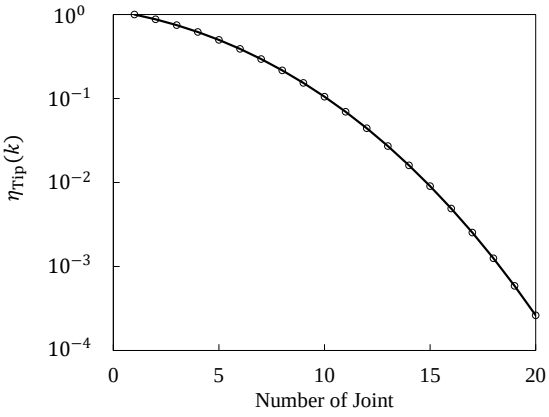

Fig. 9. Relationship between number of joints and tension transmission rate of the rope to drive the joint at the tip.

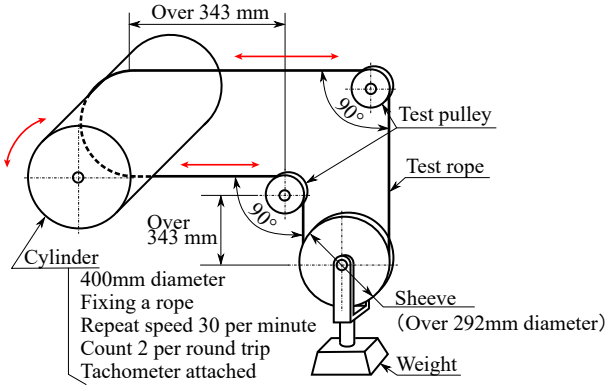

Fig. 10. Experimental system to measure reduction in rope strength due to friction.

B. Experiment Results

In order to investigate the durability of the rope in detail, we conducted 70,000 repetitions (standard) and 140,000 repetitions (doubled). Figure 11 shows the relationship between the strength of ropes and number of repetitions using free pulleys or fixed pulleys. The same graph also shows the value when testing under the conditions described in ISO 2020:1997 as a reference. The strength efficiency is the ratio of the breaking strength of the tested rope and the tensile strength of the virgin rope. Although the driving speed is different, the strength efficiencies for the free and fixed pulleys are quite similar. However, if the driving speed is set to exceed 0.686 m/s, as defined in ISO 2020:1997, the ropes break before completing 70,000 repetitions due to the accumulation of heat. In order to drive the joint quickly, we need to use Zylon or Vectran ropes, which have high durability against high temperature.

The experimental results reveal that repetitive rope sliding on a fixed pulley made of POM does not show significant strength reduction when the sliding speed is low.

V. IMPLEMENTATION TO ROBOT ARM

In this section, we show that the proposed mechanism can be used with a robot arm. Long-reach robot arms are necessary for decommissioning tasks in locations such as the Fukushima Nuclear Power Plant. The robot arms are required to be very long and must have multiple joints. Pulleys are absent, and the mechanism contains a very simple and compact joint. The proposed mechanism is thus effective for long-reach and multi-joint robot arms. We investigate the performance of a robot arm using the proposed mechanism. We develop a 3-DoF Horizontal Articulated Robot Arm, as shown in Fig. 12. Table I shows the specifications of the arm. Joint 1 is driven by a timing belt and pulley. Joints 2 and 3 are driven by antagonistic tendons that go through Joint 1. Due to the proposed mechanism, the arm is light-weight and weighs only 1.8 kg. The arm is controlled by the amount of wound rope and the joint angle. The amount of wound rope is read by the motor encoders located at the base of the arm. The joint angle is read by the encoders in the joint. EPOS2 (MAXON) was used as the motor driver. We agree with the reviewer on this point. The explanation of the driving method in the study was inadequate. The robot arm is controlled by an antagonistic wire drive using two motors in one joint. One motor winds up the rope and the other feeds the rope. Therefore, the slack of rope does not occur while rotating the joint. Because the amount of rotation of the joint can be estimated from the winding amount of the rope, it is also possible to control the robot arm. The encoder value of the motor is used to control the take-up and delivery amount of the rope. The relationship between the rotation angle of the motor θ_{motor} and the joint θ_{joint} is shown as

$$\theta_{\text{joint}} = \frac{D_{\text{motor}}}{D_{\text{joint}}}\theta_{\text{motor}} \tag{5}$$

where θ_{joint} and D_{joint} are the diameters of the pulley set at the motors and joints, respectively. The ability of the arm to conduct basic operations, expansion/storage motions, and wrap-around exploration into narrow spaces was confirmed. Fig. 13 shows top views of the expansion motions. Also, pose repeatability, position stabilization time, position overshoot, and minimum resolution were measured in order to evaluate the performance of the arm.

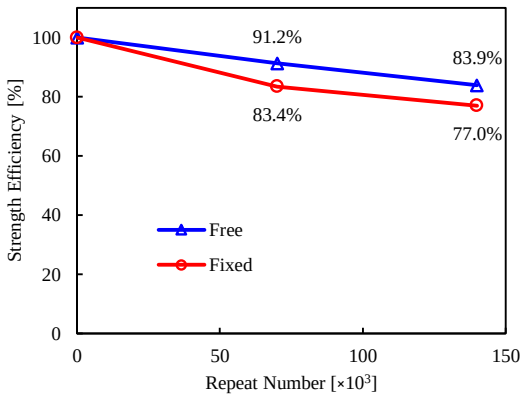

Fig. 11. Relationship between the strength efficiency of the ropes and number of repetitions when using free or fixed pulleys.

A. Experimental Setup

ISO 9283:1998 establishes the test and calculation methods for pose repeatability, position stabilization time, and position overshoot. The arm is operated repeatedly to expand/store 30 times, as shown in Fig. 13, and the tip position of the arm is measured with a laser displacement meter (LK-G32, KEYENCE). The position stabilization time is defined as the

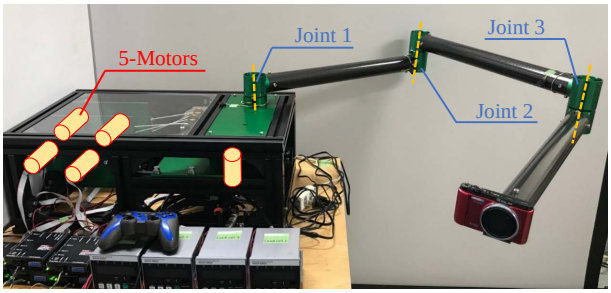

Fig. 12. Horizontal robot arm composed of three joints with the proposed mechanism.

TABLE I. Specification of the 3-DoF horizontal articulated robot arm.

Length [m]	1.8
Diameter [mm]	50
Weight [kg]	33.3 (Arm : 1.8)
DoF	3 (only yaw)
Joint movable range [deg]	±174
Actuator	maxon RE40(150 W) ×5
Joint angle meter	Rotary encoder ×3 (MES-6PST-2000,MTL)
Tension sensor	Load cell ×4 (LUR-A-SA1,KYOWA)
Rope	UHMWPE fiber rope ($\phi = 2.0$ mm)

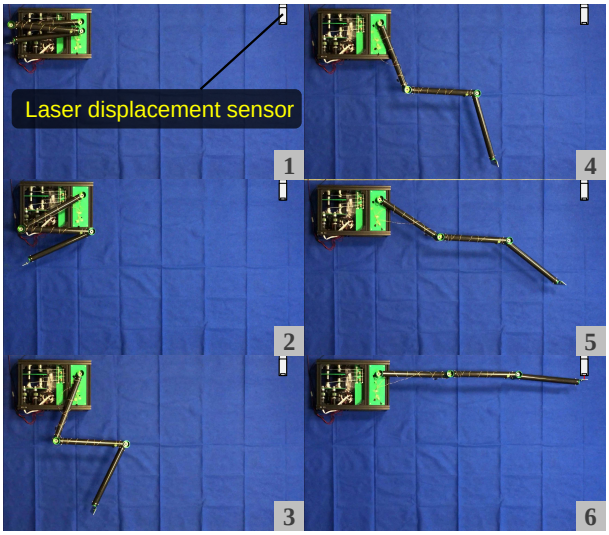

Fig. 13. Top views of arm motion when expanding and storing the arm (at approximately 2.5 s intervals).

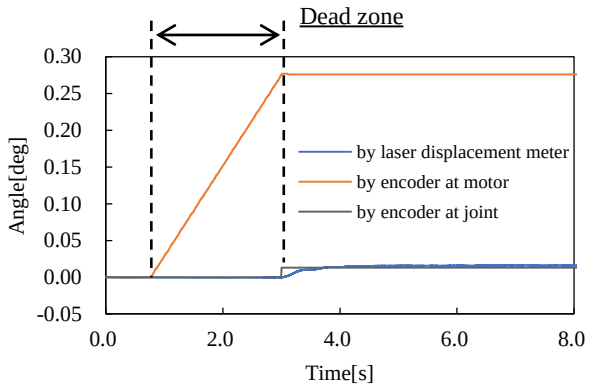

Fig. 14. Joint angle measured by a laser displacement meter and the encoder at the motor and joint while driving the motors.

time taken for the vibration to fall within ± 0.3 mm after the first vibration peak appears.

In order to investigate the control characteristics of the arm, the minimum resolution of the joint angle is measured in addition to the above three items. We control the motor in the base to drive until the joint moves and rolls up the rope. Initially, the joints do not respond immediately. Due to friction, the joints are not driven until the tension increases to a certain value. Therefore, a dead zone appears, as shown in Fig. 14. The experiment to measure the minimum resolution of the arm is conducted to investigate the size of the resolution compared to the resolution of the joint encoder (0.0135 deg). We repeat the same operation 10 times and measure the tip motion with a laser displacement meter.

B. Result

Table II shows the pose repeatability, position stabilization time, position overshoot, and minimum resolution obtained by the above experiment. The maximum values of position

TABLE II. Performance of the arm.

	Average	Maximum
Pose repeatability [mm]	0.40	-
Position stabilization time [s]	0.993 ± 0.001	0.995
Position overshoot [mm]	4.45 ± 0.04	4.52
Minimum resolution [deg]	0.059 ± 0.002	0.066

stabilization time, position overshoot, and minimum resolution are also listed in the table as references. The pose repeatability of the WAM Arm [12], a wire-driven robot arm, is reported as 0.1 mm. This robot arm can be controlled with an accuracy comparable to that of the WAM Arm, which is notable considering that the robot arm in this study is nearly twice as long as the WAM Arm. The fact that the minimum resolution is less than 0.07 deg at the most suggests the possibility of realizing control with high precision. However, the rigidity of the arm is presumed to be low given that the position stabilization is about 1 s and the overshoot is about 4.5 mm. We infer that this aspect is greatly affected by the stretching of the ropes.

VI. CONCLUSIONS

We proposed a method to relay ropes while bundling them, and termed it Bundled Wire Drive. Then, as an example, we proposed a mechanism by which multiple ropes pass through the center of a revolute joint. The reduction in the tension transmission efficiency due to friction and the lowered durability due to rope sliding were investigated using a prototype. The following results were obtained. First, the proposed mechanism can be applied to a robot arm with as many as 15 joints. Second, the rope strength is reduced by about 8% at most due to sliding. Finally, we confirmed the feasibility of the proposed mechanism by prototyping the robot arm. The basic operation was confirmed and the performance of the robot arm was evaluated. The findings revealed that pose repeatability is 0.40 mm, position stabilization time is 0.993 s, position overshoot is 4.45 mm, and minimum resolution is 0.059 deg (maximum: 0.066 deg). In our future works, we will concentrate on using the proposed BWD to improve the robot arm in terms of reach, multiple articulation, and payload at the tip. The following three investigations will also be part of our future works: (1) tension transmission efficiency in serial manipulator, (2) the durability of rope against tangential sliding and twist, and (3) the influence of lubricant on durability and transmission efficiency.

ACKNOWLEDGMENT

We would like to thank the Todoroki and Mizutani Laboratory in the School of Engineering at the Tokyo Institute of Technology, which maintains the tensile testing device that we used. We also would like to express our gratitude to Dr. Masato Kanekiyo, who measured the tensile strength of the ropes after repetitive bending. This paper is based on the results obtained from a project commissioned by the New Energy and Industrial Technology Development Organization (NEDO).

REFERENCES

[1] T. Treratanakulwong, H. Kaminaga, and Y. Nakamura, "Low-friction tendon-driven robot hand with carpal tunnel mechanism in the palm by optimal 3d allocation of pulleys," in *Robotics and Automation (ICRA), 2014 IEEE International Conference on*. IEEE, 2014, pp. 6739–6744.

[2] E. J. Hanly and M. A. Talamini, "Robotic abdominal surgery," *The American journal of surgery*, vol. 188, no. 4, pp. 19–26, 2004.

[3] A. Takata, G. Endo, K. Suzumori, H. Nabae, Y. Mizutani, and Y. Suzuki, "Modeling of synthetic fiber ropes and frequency response of long-distance cable–pulley system," *IEEE Robotics and Automation Letters*, vol. 3, no. 3, pp. 1743–1750, 2018.

[4] A. Horigome and G. Endo., "Basic study for drive mechanism with synthetic fiber rope–investigation of strength reduction by bending and terminal fixation method," *Advanced Robotics*, vol. 30, no. 3, pp. 206–217, 2016.

[5] A. Horigome and G. Endo, "Investigation of repetitive bending durability of synthetic fiber ropes," *IEEE Robotics and Automation Letters*, vol. 3, no. 3, pp. 1779–1786, 2018.

[6] A. Horigome, G. Endo, A. Takata, and Y. Wakabayashi, "Development of new terminal fixation method for synthetic fiber rope," *IEEE Robotics and Automation Letters*, pp. 4321–4328, 2018.

[7] G. Palli, M. Hosseini, and C. Melchiorri, "Twisted string actuation with sliding surfaces," in *Intelligent Robots and Systems (IROS), 2016 IEEE/RSJ International Conference on*. IEEE, 2016, pp. 260–265.

[8] B. Suthar, M. Usman, H. Seong, I. Gaponov, and J.-H. Ryu, "Preliminary study of twisted string actuation through a conduit toward soft and wearable actuation," in *2018 IEEE International Conference on Robotics and Automation (ICRA)*. IEEE, 2018, pp. 2260–2265.

[9] H. Nakamoto, J. Oga, H. Ogawa, and N. Matsuhira, "Development of wire-driven arm for human-symbotic robot," *Journal of Japan Society for Design Engineering*, vol. 50, no. 6, pp. 302–309, 2015.

[10] "OC Robotics Snake-arm robots," http://www.ocrobotics.com/products--services/ Accessed:2018-09-10.

[11] Y. Nakamura, G. Endo, K. Suzumori, and A. Horigome, "A proposal of bundled wire drive -wire relay mechanism that allows the twist and sliding contact of the wires-," in *Proc. JSME Conf. Robot. Mecha.*, 2016, pp. 2P1–14b4.

[12] "Barrett Technology Inc. WAM Arm," http://www.barrett.com/robot/products-arm.htm Accessed:2018-09-10.